Annals of Mathematics and Computer Science ISSN: 2789-7206
Vol 25 (2024) 1-18 https://doi.org/10.56947/amcs.v25.361

MATHEMATICAL ANALYSIS OF THE EFFECTS OF PRECARIOUS HEALTH SYSTEM ON COVID-19 TRANSMISSION DYNAMICS: CASE OF BURKINA FASO

OUSMANE KOUTOU[1*], KOMI AFASSINOU[2], ADAMA OUEDRAOGO[3], AND ABOU BAKARI DIABATE[4]

Abstract. In the early moments of the pandemic of coronavirus disease 2019 (COVID-19), the level of effectiveness in treatment and management of patients was limited due to the lack of effective medications and adapted infrastructures in several countries especially in most developing countries. In this study, we propose an SIR-pattern model to investigate the epidemiological effect of delay in hospitalization and case managements. After computing the basic reproduction number thanks to the Next Generation Matrix method, we proved that the model has a locally asymptotically stable disease-free equilibrium whenever the basic reproduction number is less than one, and condition which ensure the appearance of two endemic equilibria indicating the possibility of having backward bifurcation is determined. When the basic reproduction number exceeds one, Lyapunov functional technique is used to establish the global stability of the unique endemic equilibrium point. Also, we presented a local sensitivity analysis that gives better understanding of the role of each model parameter appearing in the basic reproduction number. Numerical simulation of the model is also performed to corroborate the analytical results. Finally, we fitted our model by using reported data for Burkina Faso, and the results showed that it can be used for predicting the disease outcomes.

1. Introduction and preliminaries

The COVID-19 pandemic has threatened to collapse hospital and intensive care services, and has affected care programs for both COVID-19 and non-COVID-19 patients. Epidemic activity was not constant, but was concentrated in some waves, which were artificially broken by lockdowns and other social distancing measures [1, 3, 13]. Moreover, since the outbreak of disease, researchers have put their energy to finding ways on how to control the pandemic. Therefore, apart from the stay-at-home, the contact tracing and the isolation of infected individuals, several other control measures have been explored such that awareness campaigns through media coverage [15, 25, 30], the use of some imperfect vaccines, treatment, etc [15, 21, 39]. Meanwhile, it should be noted that COVID-19

Date: Received: Jul 29, 2024; Accepted: Sep 22, 2024.
* Corresponding author.
2010 *Mathematics Subject Classification.* 34D20, 34D23, 34D45, 37C75.
Key words and phrases. COVID-19, Health system weakness, Stability analysis, Fitting, Numerical simulations.

has not affected all hospital services to the same extent. In France, for example, the most requested hospital activities in 2020 were the digestive care and orthopaedic trauma services, which together account for a quarter of total hospitalizations. While COVID-19, being a respiratory disease, has mainly affected the pulmonology department, as well as resuscitation for those with severe forms of the disease [4, 26, 28]. If we look at these services, we see that the impact of COVID-19 is much greater than what the total hospitalizations given in a report from the Technical Information Agency on hospitalization might lead us to believe. Thus, coronavirus patients represented 18% of hospital stays in intensive care and in pulmonology departments, while the impact of the epidemic was concentrated mainly over two months, [3, 25, 27].

As for Burkina Faso, when the first case of COVID-19 was reported on March 9, 2020, the country had already been experiencing a complex humanitarian and security crisis for more than 5 years [2, 16, 21]. The increase in violence and insecurity caused by armed insurgent groups is now disrupting the lives of about 2.2 million people and has resulted in the displacement of more than a million civilians. In a context where populations have fled conflict zones, the demand for health services has continued to grow, as attacks have reduced the number of operational health facilities [4, 16, 17]. In September 2020, in fact, 95 health establishments were closed, or 85% of the infrastructures in the 6 regions hit by insecurity. Weaknesses in the health system, notably due to poor data management and the overall inadequacy of emergency health services, including for the COVID-19 response, have prevented the provision of good quality health services [2, 20, 38]. Motivated by the aforesaid studies, in this work we propose and examine a new mathematical model with a saturated treatment rate to better understand the consequences related to the delay in care due to the weakness of health system in general and more accurately in Burkina Faso, during the pandemic of COVID-19.

Several mathematical studies have taken into account the saturation of treatments in COVID-19 case due to varied reasons from one geographical area to another. Indeed, R. T. Alqahtani et al. in [6] analysed the dynamics of COVID-19 in Saudi Arabia using a mathematical model with a constant vaccination rate, a saturated treatment function and a saturated incidence rate. Their SEIR-type model was fitted to the spread of COVID-19 using data collected in Saudi Arabia. They showed that their model can exhibit both Hopf and backward bifurcation, and studied the effects of the vaccination rate and treatment function parameters on the disease dynamics. J. K. Ghosh et al. in [14] proposed a epidemiological model of SEQIR-type to describe the dynamics of COVID-19 in Italy. Infections occur according to a standard incidence function, and they use a saturated treatment rate to take into account the limitation of patient care due to the rapidity of infections. They perform an optimal control study to evaluate the impacts of adapting lockdowns to maintain social distancing on the dynamics of the pandemic. Also, Furthermore, D. A. Oluyori et al. in [32], carried out a Backward and Hopf bifurcation study of a SEIRS-type model of the COVID-19 epidemic. They use a saturated incidence function and a saturated treatment response, due to the limited availability of medical resources favoring the emergence of complex

dynamics that complicate disease control. The parameter values used for the numerical simulations were adapted in reported data in Nigeria during COVID-19 pandemic outbreak. In addition, P. Saha et al. in [35], developed a SEQAIHR-type model adjusted with real data of COVID-19 infection in Hong Kong from December 19, 2021 to April 3, 2022. Due to limited medical facilities, they used saturated treatment. A mathematical study of the model was carried out for a better understanding of COVID-19 transmission in Hong Kong in 2022, and for the development of optimal control strategies considering vaccination and saturated treatment of hospitalized people. Other mathematical studies have tried to highlight various aspects during COVID-19 disease manifestation in several countries, sometimes using saturated incidence functions and/or saturated treatments. We have designed in this manuscript, a simple mathematical model of the SIR type for COVID-19 dynamics, which particularity mainly lies in the following points:

- the inclusion of a proportion p of immunised individuals in the recruitment,
- infections occur through a linear incidence function,
- symptomatic and asymptomatic infectious persons are considered in the same compartment I,
- consideration of a saturated treatment of symptomatic hospitalized people in order to take into account the weakness of health systems in the face of the COVID-19 pandemic,
- taking into account natural recovery with good immunity against the virus through the parameter γ,
- consideration of a parameter δ to take account of naturally recovered individuals with low immunity against the coronavirus and/or people wrongly diagnosed as having COVID-19,
- the model is fitted with real data collected in Burkina-Faso during the COVID-19 pandemic, from 11 March to 14 December 2020.

After this short introduction to set the context, the rest of the paper is organized as follows: Section 2 is devoted to the model formulation. In Section 3, we proposed some mathematical analysis of the model; more precisely, we assess the well-posedness, the stability results of the steady states, the bifurcation and sensibility analysis of the model parameters according to the basic reproduction number. In Section 4 is proposed some data fitting and numerical simulation in order to corroborate our theoretical results and also to make the model useful for predicting the disease outcomes. And Section 5 is meant for concluding remarks.

2. Model formulation

In this work, we have split the human population into three states that is, susceptible persons $S(t)$, COVID-19 infectious individuals $I(t)$ and the compartment $R(t)$ of COVID-19 cured and immunised persons. Therefore, the human total population is given by $N(t) = S(t) + I(t) + R(t)$. All the model parameters are non-negative and defined as follows: Λ is the recruitment rate (newborns and immigrants) with a proportion p of people immunised against COVID-19; β is the

disease transmission rate; δ is the rate of infectious persons that, after recovering without treatment, become susceptible due to a low immunity; γ is the rate of infectious people recovered without treatment with a certain immunity against COVID-19, and then enter the immunized compartment; the disease induced mortality rate is d ; μ is the natural mortality rate; ρ represents the saturation factor, measuring the effect of a delayed in patients management in hospitals; r is the cure rate by treatment when there is no delay in the management of infected people in hospital, $\rho = 0$, and $r/(1+\rho I)$ is the cure rate for any value of ρ. The quantity $\mathscr{F}(I) = rI/(1+\rho I)$ represents the number of people cured by treatment and tends to r/ρ when a very large number of people is infected, these people enter the compartment of cured and immunised people [31, 33]. The flowchart of the model is illustrated by Figure 1, from which we draw the model system (2.1).

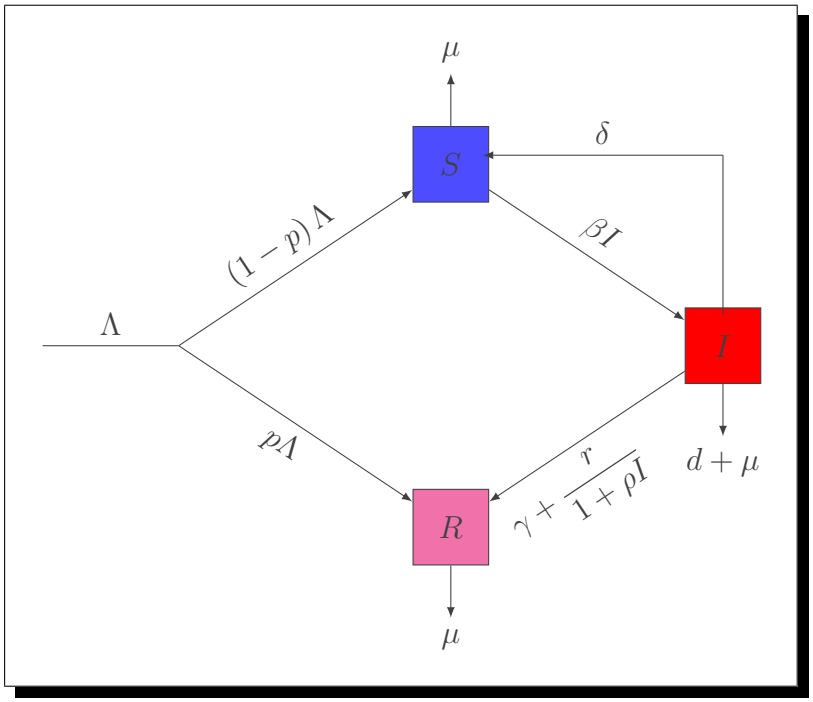

FIGURE 1. Compartmental representation of the COVID-19 transmission dynamics.

$$\begin{cases} S' = (1-p)\Lambda + \delta I - \beta SI - \mu S \\ I' = \beta SI - (\delta + \gamma + d + \mu)I - \mathscr{F}(I) \\ R' = p\Lambda + \gamma I + \mathscr{F}(I) - \mu R. \end{cases} \tag{2.1}$$

3. Mathematical analysis

3.1. **Well-posedness.**

- **Existence and uniqueness of solutions**

  Let $X(t) = (S, I, R)$. The initial conditions problem with respect to system (2.1) reads as follows

$$\begin{cases} X'(t) = \mathcal{G}(X(t)), \\ X(t_0) = X_0, \end{cases} \tag{3.1}$$

  where the function $\mathcal{G}(X(t))$ is the right hand side of system (2.1).

  Since $\mathcal{G}(X(t))$ is $\mathcal{C}^\infty$, it is locally Lipschitzian on $\mathbb{R}^3$. Therefore, the existence and the uniqueness of the Cauchy problem (3.1) is ensured by Cauchy-Liptchitz's theorem [40, 36, 41].

- **Positivity of solutions**

  In this part, we prove that under non-negative initial conditions, the model solutions are positive.

  Theorem 3.1. *Consider $S_0 \geq 0,\ I_0 \geq 0,\ R_0 \geq 0$. The solution of system (2.1) with respect to $(S(0), I(0), R(0)) = (S_0, I_0, R_0)$ is non-negative, that is, $S(t) \geq 0, I(t) \geq 0, R(t) \geq 0$ for $t > 0$.*

  Proof. Let $X(t) = (S(t), I(t), R(t))$ be the solution of (2.1) under initial non-negative conditions $X_0 = (S(0), I(0), R(0)) = (S_0, I_0, R_0)$.

  By the continuity of solution, for all $S(t), I(t), R(t)$ that have positive initial condition values at $t = 0$, we have the existence of an interval $(0, t_0)$ such that $S(t) \geq 0, I(t) \geq 0, R(t) \geq 0$ for $0 < t < t_0$. We will prove that $t_0 = \infty$.

  If $S(t_1) = 0$ for $t_1 \geq 0$ and $I(t),\ R(t)$ stay positive at $t = t_1$, then

$$S'(t)|_{t=t_1} = (1-p)\Lambda + \delta I(t_1) \geq 0.$$

  This ensures that at any time the solution reaches the axis, its derivative increases, and the function $S(t)$ does not cross to negative part.

  Similarly,

$$I(t_1) = 0 \text{ implies that } I'(t)|_{t=t_1} = 0,$$

  and

$$R(t_1) = 0 \text{ leads to } R'(t)|_{t=t_1} = p\Lambda + \gamma I(t_1) + \frac{rI(t_1)}{1+\rho I(t_1)} \geq 0$$

  Therefore, $X(t)$ never crosses the axes $S = 0, I = 0, R = 0$ when it touches them. Thus, for any non-negative initial conditions, all equation solutions remain non-negative. □

Theorem 3.2. *Let $(S(t), I(t), R(t))$ be the solution of system (2.1) with the initial conditions (S_0, I_0, R_0). The compact set*

$$\Gamma = \left\{ (S(t), I(t), R(t)) \in \mathbb{R}^3_+ : 0 \leq S(t) + I(t) + R(t) \leq \frac{\Lambda}{\mu} \right\}$$

containing it, is positively invariant and attracts all positive orbits in $\mathbb{R}_+$.

Proof. Indeed, $N'(t) = \Lambda - \mu N(t) - dI(t) \leq \Lambda - \mu N(t)$ since $dI(t) \geq 0$. Thanks to Birkhoff and Rota theorem [8, 37, 42], $0 \leq N(t) \leq \dfrac{\Lambda}{\mu}$. Hence, the set Γ is positively invariant and attractive for model (2.1). □

3.2. **Model steady states.** The model (2.1) admits a unique infection-free equilibrium given as

$$\mathcal{E}^0 = \left(\frac{(1-p)\Lambda}{\mu}, 0, \frac{p\Lambda}{\mu} \right). \tag{3.2}$$

And, thanks to the next-generation matrix, we get the basic reproduction number

$$\mathcal{R}_0 = \frac{\beta(1-p)\Lambda}{\mu\left(\delta+\gamma+d+\mu+r\right)}. \tag{3.3}$$

Putting the right-hand side of the system (2.1) to zero, one obtains the endemic equilibrium point as

$$\mathcal{E}^* = \left(\frac{(1-p)\,\Lambda + \delta I^*}{\mu + \beta I^*}, I^*, \frac{p\Lambda + \gamma I^*}{\mu} + \frac{rI^*}{\mu\left(1+\rho I^*\right)} \right) \tag{3.4}$$

where I^* satisfies the following quadratic equation

$$a(I^*)^2 + bI^* + c = 0, \tag{3.5}$$

with

$$\begin{aligned} a &= \beta\left(\gamma+d+\mu\right)\rho, \\ b &= \left(\delta+\gamma+d+\mu\right)\left(\beta+\mu\rho\right) + r\beta - \beta(1-p)\rho\Lambda - \beta\delta, \\ c &= \mu\left(\delta+\gamma+d+\mu+r\right)\left(1-\mathcal{R}_0\right). \end{aligned}$$

As $a > 0$, knowledge of the sign of b, c and $\Delta = b^2 - 4ac$ is necessary to determine the number of endemic equilibria. The value of $\mathcal{R}_0$ which sets Δ to zero denoted $\mathcal{R}_0^C$ is given by:

$$\mathcal{R}_0^C = 1 - \frac{b^2}{4\mu a\left(\delta+\gamma+d+\mu+r\right)}.$$

The different cases are then summarised as follows:

Theorem 3.3. *Model (2.1) admits :*

- (*i*) *a unique endemic equilibrium if* $c < 0$ (*i.e.* $\mathcal{R}_0 > 1$),
- (*ii*) *a unique endemic equilibrium if* $c = 0$ (*i.e.* $\mathcal{R}_0 = 1$) *and* $b < 0$,
- (*iii*) *a unique endemic equilibrium if* $c > 0$ (*i.e.* $\mathcal{R}_0 < 1$), $b < 0$ *and* $\Delta = 0$ (*i.e.* $\mathcal{R}_0 = \mathcal{R}_0^C$),
- (*iv*) *two endemic equilibria if* $c > 0$ (*i.e.* $\mathcal{R}_0 < 1$), $b < 0$ *and* $\Delta > 0$ (*i.e.* $\mathcal{R}_0 > \mathcal{R}_0^C$),
- (*v*) *no endemic equilibrium in all the other cases.*

3.3. **Stability results of the infection-free point.**

3.3.1. *Local stability of* $\mathcal{E}^0$. At the infection-free equilibrium, the Jacobian matrix is given by

$$\mathcal{M}_0 = \begin{pmatrix} -\mu & -\dfrac{\beta(1-p)\Lambda}{\mu} + \delta & 0 \\ 0 & (\delta+\gamma+d+\mu+r)(\mathcal{R}_0-1) & 0 \\ 0 & \gamma+r & -\mu \end{pmatrix} \tag{3.6}$$

and then the characteristic polynomial is given as follows

$$P(\lambda) = \det(\mathcal{M}_0 - \lambda I_3) = (\lambda+\mu)^2\left((\delta+\gamma+d+\mu+r)(\mathcal{R}_0-1) - \lambda\right).$$

That leads to the following eigenvalues: $\lambda = -\mu$ or $\lambda = (\delta+\gamma+d+\mu+r)(\mathcal{R}_0-1)$. Therefore, the following result holds

Theorem 3.4. *If* $\mathcal{R}_0 < 1$*, then the infection-free equilibrium* $\mathcal{E}^0$ *is locally asymptotically stable.*

3.3.2. *Global stability of* $\mathcal{E}^0$. In order to analyse the global stability of $\mathcal{E}^0$, we consider the following threshold parameter

$$\mathscr{R}_0^* = \frac{\beta\Lambda}{\mu\left(\delta+\gamma+d+\mu+\left(\dfrac{r}{1+(\rho\Lambda/\mu)}\right)\right)}.$$

It is easy to see that

$$\mathcal{R}_0 < \mathscr{R}_0^*, \quad \text{so} \quad \mathscr{R}_0^* < 1 \Longrightarrow \mathcal{R}_0 < 1.$$

Theorem 3.5. *If* $\mathscr{R}_0^* < 1$ *the infection-free equilibrium is globally asymptotically stable in* Γ.

Proof. From $\mathscr{R}_0^* < 1$, we have

$$\frac{\beta\Lambda}{\mu} - (\delta+\gamma+d+\mu) - \frac{r}{1+(\rho\Lambda/\mu)} < 0.$$

By considering the infected compartment, let consider this Lyapunov candidate

$$\mathscr{L}_1 = I \tag{3.7}$$

It is obvious to see that $\mathscr{L}_1$ is equal to zero at $\mathcal{E}^0$ and positive elsewhere. Also,

$$\mathscr{L}_1' = I' = \beta SI - (\delta+\gamma+d+\mu)I - \frac{rI}{1+\rho I}.$$

Since $N \leq \dfrac{\Lambda}{\mu}$, then $S \leq \dfrac{\Lambda}{\mu}$ and $I \leq \dfrac{\Lambda}{\mu}$. Thus

$$\mathscr{L}_1' \leq \left(\frac{\beta\Lambda}{\mu} - (\delta+\gamma+d+\mu) - \frac{r}{1+(\rho\Lambda/\mu)}\right) I \leq 0.$$

Furthermore $L' = 0$ if and only if $I = 0$. The largest compact invariant set in $\{(S,I,R) \in \Gamma / \mathscr{L}_1' = 0\}$ is the singleton $\{\mathcal{E}^0\}$. Therefore, by the Lasalle-Lyapunov theorem [18, 24], every solution that starts in Γ approaches $\mathcal{E}^0$ as $t \longrightarrow \infty$. Then $\mathcal{E}^0$ is globally asymptotically stable whenever $\mathscr{R}_0^* < 1$. □

3.4. **Bifurcation analysis.** Forward and backward bifurcation play an important role in epidemic models. As for forward bifurcation with respect to $\mathcal{R}_0$ occurs when near the critical value $\mathcal{R}_0 = 1$, for $\mathcal{R}_0 < 1$ only the disease-free equilibrium exists and it is locally asymptotically stable, while for $\mathcal{R}_0 > 1$ besides the disease-free equilibrium, which is unstable, there exists a locally asymptotically stable endemic equilibrium [12, 22, 30]. Yet, backward bifurcation with respect to $\mathcal{R}_0$ occurs when near the critical value $\mathcal{R}_0 = 1$, for $\mathcal{R}_0 < 1$ besides the disease-free equilibrium, which is locally asymptotically stable, there exists an endemic equilibrium which is unstable, while for $\mathcal{R}_0 = 1$ the endemic equilibrium collides with the disease-free equilibrium and disappears while the disease-free equilibrium becomes unstable for $\mathcal{R}_0 > 1$. When backward bifurcation occurs, even if control measures reduce $\mathcal{R}_0$ slightly below one, the disease will not disappear by itself. Additional effort is necessary for the elimination of the disease [9, 12, 37]. Due to the importance of this phenomenon to epidemic modelling, numerous of methods that give necessary and sufficient conditions in ODE models have been proposed [5, 29]. Most important of those is a result based on the Center Manifold Theory that provides criteria to derive conditions for backward bifurcation [9, 10, 12, 30]. In this study, the conditions $\mathcal{R}_0 < \mathcal{R}_0^C < 1$ or $\mathcal{R}_0 = 1$ and $b > 0$ are necessary to eradicate the disease. Moreover, by using the central manifold theory, we draw sufficient conditions to obtain a backward bifurcation when $\mathcal{R}_0 = 1$.
Let $x_1 = S$, $x_2 = I$, $x_3 = R$, $x = (x_1, x_2, x_3)^T$, model (2.1) can be rewritten

$$\begin{cases} x_1' &= f_1(x) = (1-p)\Lambda - \beta x_1 x_2 + \delta x_2 - \mu x_1 \\ x_2' &= f_2(x) = \beta x_1 x_2 - \delta x_2 - \gamma x_2 - d x_2 - \dfrac{r x_2}{1+\rho x_2} - \mu x_2 \\ x_3' &= f_3(x) = p\Lambda + \gamma x_2 + \dfrac{r x_2}{1+\rho x_2} - \mu x_3 \end{cases} \tag{3.8}$$

or using the simple expression

$$x' = f(x), \;\; f = (f_1, f_2, f_3).$$

Consider now the situation where $\mathcal{R}_0 = 1$, and by considering $\beta = \beta^*$ as the bifurcation parameter, we obtain

$$\beta^* = \frac{\mu\,(\delta + \gamma + d + \mu + r)}{(1-p)\Lambda}.$$

The Jacobian matrix $\mathcal{M}_0$ at the infection-free equilibrium $\mathcal{E}^0$ given above, and denoted $\mathcal{M}_0^*$ when $\beta = \beta^*$, has a simple zero eigenvalue and the real part of each of the other eigenvalues is negative. Therefore, the model (2.1) dynamics can be analysed using the central manifold theory [9, 10, 12, 30]. Particularly, we apply Theorem 7, in [30], also stated in [10]. Consider $w = (w_1, w_2, w_3)^T$ a right eigenvector corresponding to the zero eigenvalue of $\mathcal{M}_0^*$ i.e. $\mathcal{M}_0^* w = 0$. The calculation gives

$$w_1 = -\frac{(\gamma + d + \mu + r)w_2}{\mu}, \;\; w_2 = w_2 \text{ and } w_3 = \frac{(\gamma + r)w_2}{\mu}.$$

Also, suppose that $v = (v_1, v_2, v_3)$ is a left eigenvector corresponding to the zero eigenvalue of $\mathcal{M}_0^*$, i.e. $v\mathcal{M}_0^* = 0$, we obtain

$$v_1 = 0,\ v_2 = v_2 \text{ and } v_3 = 0.$$

Now, we have to calculate

$$\mathscr{A} = \sum_{k,i,j=1}^{3} v_k w_i w_j \frac{\partial^2 f_k}{\partial x_i \partial x_j}\left(\mathcal{E}^0, \beta^*\right) \text{ and } \mathscr{B} = \sum_{k,i=1}^{3} v_k w_i \frac{\partial^2 f_k}{\partial x_i \partial \beta_M}\left(\mathcal{E}^0, \beta^*\right).$$

Rigorous computations give

$$\mathscr{A} = 2v_2 w_2^2 r\rho\,(1-\mathscr{R}) \text{ and } \mathscr{B} = \frac{(1-p)v_2 w_2 \Lambda}{\mu} > 0,$$

where

$$\mathscr{R} = \frac{(\gamma + d + \mu + r)(\delta + \gamma + d + \mu + r)}{(1-p)r\rho\Lambda}.$$

Thus we can draw the following result

Theorem 3.6. *Model (2.1) undergoes a backward bifurcation at $\mathcal{R}_0 = 1$ whenever $\mathscr{A} > 0$ (i.e. $\mathscr{R} < 1$) and a forward bifurcation whenever $\mathscr{A} < 0$ (i.e. $\mathscr{R} > 1$).*

We have presented in the Figure 2 the curves illustrating the bifurcation phenomenon of model (2.1). The values (of the parameters) common to the two Sub-figures are: $p = 0.4,\ \delta = 0.42,\ \mu = 0.0425,\ \gamma = 2/7,\ d = 0.1746,\ r = 2.5,\ \rho = 0.12,\ v = 1$ and $w_3 = 1$. On the one hand, taking $\Lambda = 100$ and $\beta = 0.00229$, we have obtained $\mathscr{A} = 0.2574 > 0$ and $\mathscr{B} = 1411.76 > 0$, the conditions of the backward bifurcation being satisfied, Sub-figure (a) is obtained. On the other hand, the forward bifurcation presented by Sub-figure (b) is obtained for $\Lambda = 57$ and $\beta = 0.004299$, the calculation gives $\mathscr{A} = -0.001057 < 0$ and $\mathscr{B} = 804.7059 > 0$. These two Sub-figures allow us to illustrate Theorem 3.6

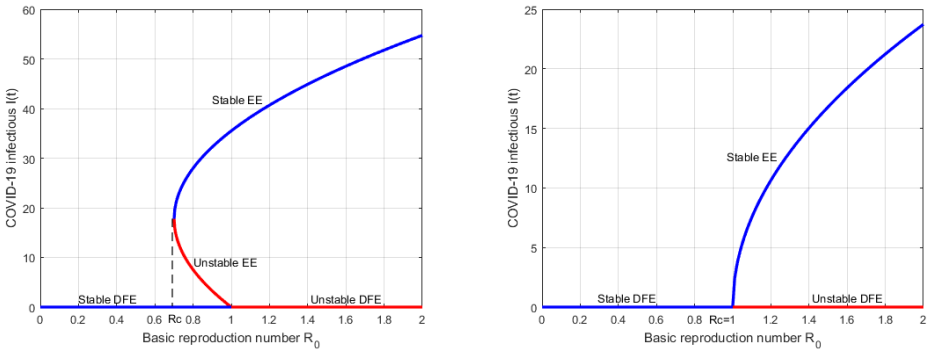

Sub-figure (a) **Sub-figure (b)**

FIGURE 2. Simulation of model (2.1) to illustrate the occurrence of backward and forward bifurcations.

Theorem 3.7. *The endemic steady state of model (2.1) existing at $\mathcal{R}_0 > 1$ is globally stable in the interior of Γ.*

Proof. The proof is based on using Lyapunov function. Consider the following Lyapunov candidate:

$$\mathscr{L}_2(S,I,R) = \frac{1}{2}\left[(S-S^*)+(I-I^*)+(R-R^*)\right]^2 \tag{3.9}$$

It is clear that for all $(S,I,R) \in (\mathbb{R}^3_+)^*$, $\mathscr{L}_2(S,I,R) > 0$ and $\mathscr{L}_2(S^*,I^*,R^*) = 0$. Now, the derivative of $\mathscr{L}_2$ is giving by

$$\begin{aligned}
\mathscr{L}_2'(S,I,R) &= \left[(S+I+R)-(S^*+I^*+R^*)\right](S+I+R)' \\
&= (N-N^*)(\Lambda-\mu N-dI) \\
&\leq (N-N^*)(\Lambda-\mu N) \text{ since } dI \geq 0 \\
&= -\mu(N-N^*)\left(N-\frac{\Lambda}{\mu}\right) \\
&\leq -\mu(N-N^*)^2 \text{ since } N^* \leq \frac{\Lambda}{\mu} \\
\mathscr{L}_2'(S,I,R) &\leq 0.
\end{aligned}$$

Also, if $\mathcal{R}_0 > 1$, $\mathscr{L}_2'(S,I,R) = 0 \Longleftrightarrow (S,I,R) = (S^*,I^*,R^*) = \mathcal{E}^*$.

Consequently, the endemic equilibrium $\mathcal{E}^*$ is globally asymptotically stable in the interior of Γ, when $\mathcal{R}_0 > 1$ [11, 21, 23, 24]. □

3.5. **Sensitivity analysis of $\mathcal{R}_0$.**

3.5.1. *Sensitivity indices and diagram.* Performing a sensitivity analysis helps us to understand how changes in the model parameters will affect the disease spreading dynamics [12, 19, 34]. And to carry out the local sensitivity analysis, a simple approach is used to calculate the sensitivity index of each parameter that appeared in $\mathcal{R}_0$ through out of the following formula [7, 21]:

$$\chi_\kappa^{\mathcal{R}_0} = \frac{\partial \mathcal{R}_0}{\partial \kappa} \times \frac{\kappa}{\mathcal{R}_0} \simeq \frac{\%\Delta\mathcal{R}_0}{\%\Delta\kappa}.$$

Therefore,

$$\chi_\beta^{\mathcal{R}_0} = \chi_\Lambda^{\mathcal{R}_0} = 1,\ \chi_p^{\mathcal{R}_0} = -\frac{p}{1-p},\ \chi_\delta^{\mathcal{R}_0} = -\frac{\delta}{\delta+\gamma+d+\mu+r},\ \chi_\gamma^{\mathcal{R}_0} = -\frac{\gamma}{\delta+\gamma+d+\mu+r}$$

$$\chi_d^{\mathcal{R}_0} = -\frac{d}{\delta+\gamma+d+\mu+r}, \chi_\mu^{\mathcal{R}_0} = -\frac{\delta+\gamma+d+2\mu+r}{\delta+\gamma+d+\mu+r},\ \chi_r^{\mathcal{R}_0} = -\frac{r}{\delta+\gamma+d+\mu+r}.$$

From the expressions of the sensitivity indices and the parameter values (see Table 1), we computed their values given in Table 1, and we also illustrated them by the the diagram of Figure 3.

These results can be interpreted as follows: $\chi_\mu^{\mathcal{R}_0} = -1,0124$ means that a 1% increase in μ will lead to 1.0124% decrease in $\mathcal{R}_0$, $\chi_\beta^{\mathcal{R}_0} = +1$ means that 1% of increase in β will produce 1% of increase in $\mathcal{R}_0$, etc.. Thus, the parameters which have a greater influence on $\mathcal{R}_0$ are μ, β, Λ, r and p, so the control methods must be implemented in order to modify them accordingly [7, 21].

Parameters	Values	References	Dimensions	Sensitivity indices
Λ	100	variable	humans/day	$+1$
β	0.0062	assumed	day^{-1}	$+1$
d	0.1746	[19]	day^{-1}	-0.0510
γ	2/7	[13, 21]	day^{-1}	-0.0835
δ	0.42	[21]	day^{-1}	-0.1227
p	0.4	assumed	day^{-1}	-0.6667
r	2.5	[41, 42]	day^{-1}	-0.7304
μ	0.0425	[12]	day^{-1}	-1.0124

TABLE 1. Parameter values and sensitivity indices for $\mathcal{R}_0$.

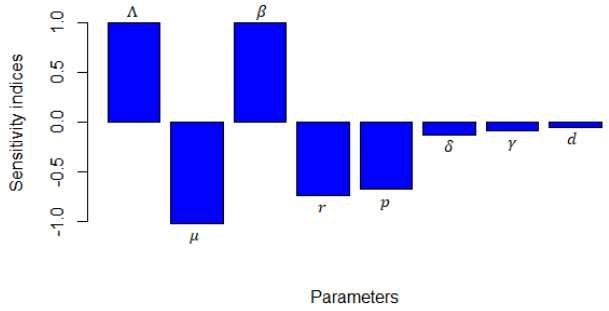

FIGURE 3. Diagram of local sensitivity indices with respect to $\mathcal{R}_0$.

3.5.2. *Illustration of some parameters effect on* $\mathcal{R}_0$. Figure 4 and 5 give the evolution of the basic reproduction number in 3D according to some of the model parameter values when it is less or greater than unity, respectively.

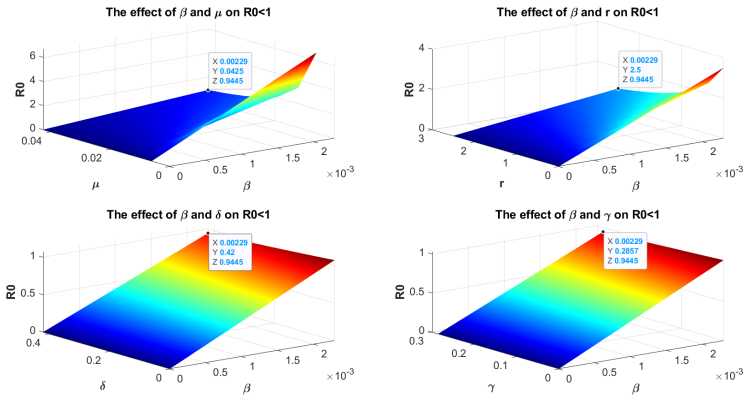

FIGURE 4. Evolution of $\mathcal{R}_0 < 1$ according to some of the model parameters in 3D.

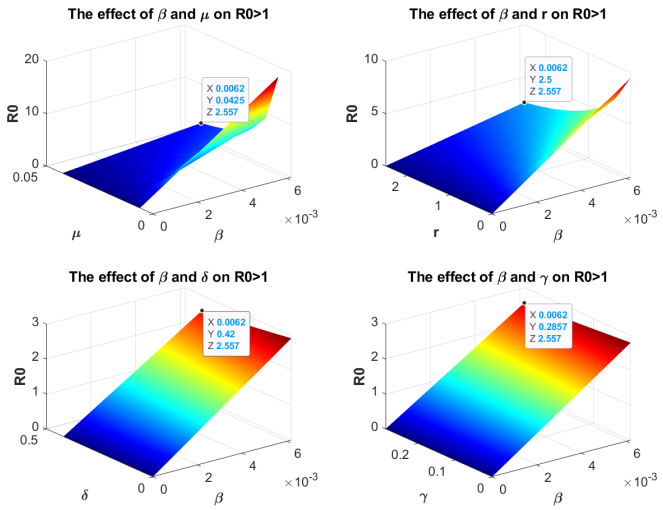

FIGURE 5. Evolution of $\mathcal{R}_0 > 1$ according to some of the model parameters in 3D.

4. Data fitting and numerical results

4.1. **Data fitting.** In this part, our main aim is to verify the validity of our model by only fitting the number of confirmed cases and the number of death in Burkina Faso given in Table 2. The data used are those collected by the health services of Burkina Faso as soon as the first cases appeared and are available on line in the COVID-19 statistics [1, 4]. The parameters have been estimated using the least squares method, a standard model fitting technique well known for its efficiency and reliability [7, 26, 31], which we ran on Matlab software and the numerical result is given by Figure 6. This method minimises the sum of squares of errors, between the collected data A_i and the values estimated in the implementation of the method B_i. The mathematical expression of the sum of squares of errors [7, 26], denoted here $\mathscr{S}$, is :

$$\mathscr{S} = \sum_{i=1}^{n} (A_i - B_i)^2.$$

4.2. **Numerical results.** In this subsection, we performed some numerical simulations for model system (2.1) by considering three main cases:

- **First case**: setting $\rho = 0.12$ and considering some parameter values that lead to $\mathcal{R}_0 < 1$ one can see that the infection-free equilibrium $\mathcal{E}^0$ is stable (see Figure 7). This corroborates Theorem 3.4 and 3.5, respectively.
- **Second case**: fixing $\rho = 0.29$ and using some parameter values that give $\mathcal{R}_0 < 1$; then we observe that besides the infection-free equilibrium $\mathcal{E}^0$ which is locally asymptotically stable we have an endemic equilibrium which is unstable. This is the occurrence of backward bifurcation that is illustrated by Figure 8. As for Figure 9, it corroborates Theorem 3.3 and 3.6, respectively.

Days	Total cases	Total Deaths
Mar. 11th 2020	2	0
Mar. 18th 2020	27	1
Apr. 2nd 2020	288	16
May 6th 2020	729	48
Jun. 1st 2020	847	53
Jul. 9th 2020	1005	53
Aug. 10th 2020	1204	54
Sep. 14th 2020	1717	56
Sep. 30th 2020	2056	58
Oct. 31st 2020	2500	67
Nov. 30th 2020	2886	68
Dec. 14th 2020	4209	71

TABLE 2. Fitted table of confirmed cases in Burkina Faso [1, 4].

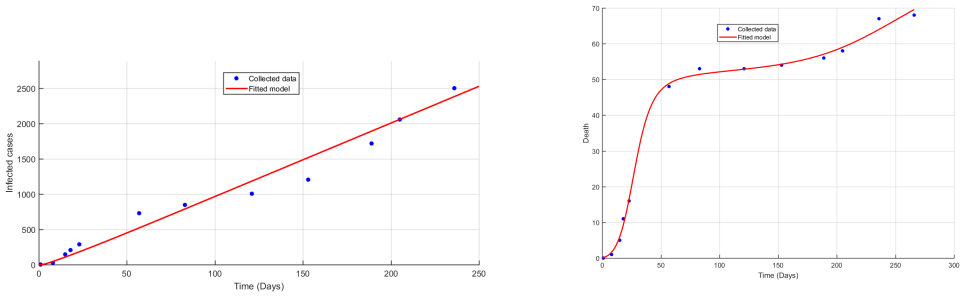

(a) (b)

FIGURE 6. Fitting curves of confirmed and death cases using data from Burkina Faso.

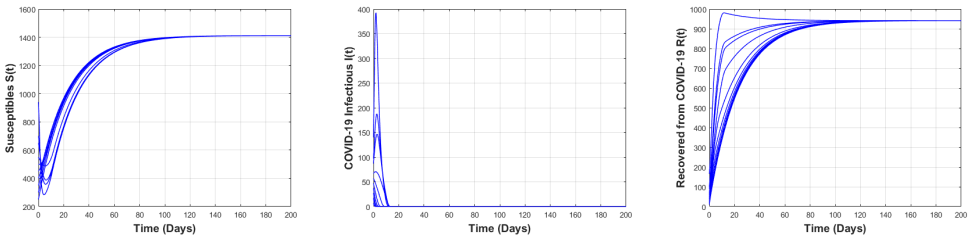

FIGURE 7. Simulations of model (2.1) with $\beta = 0.00229$ and $\rho = 0.12$, thus we obtain $\mathcal{R}_0 = 0.9445$.

• **Third case**: in the case we fix $\rho = 1.25$ and we use some parameter values that lead to $\mathcal{R}_0 > 1$; therefore, we observe that the endemic $\mathcal{E}^*$ is stable and this corroborate Theorem 3.7.

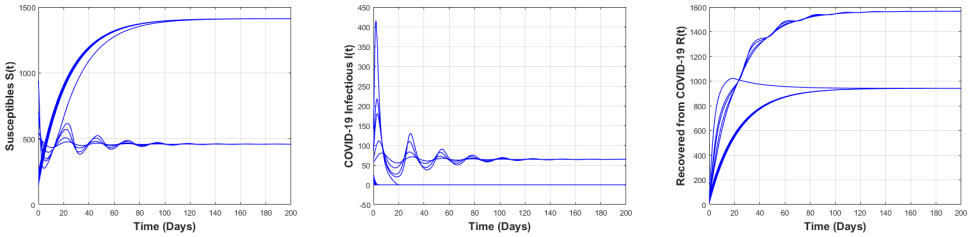

FIGURE 8. Simulations of model (2.1) with $\beta = 0.00229$ and $\rho = 0.29$, so that $\mathcal{R}_0 = 0.9445$.

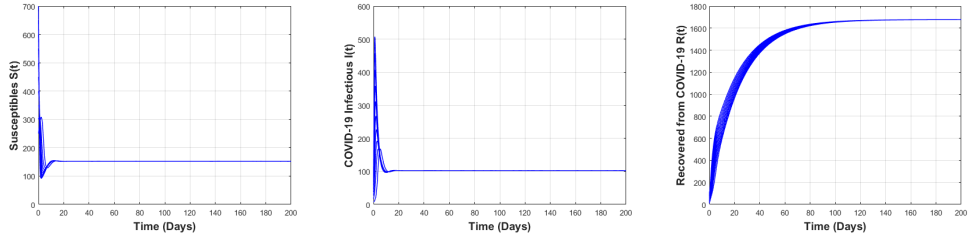

FIGURE 9. Simulations of model (2.1) with $\beta = 0.0062$ and $\rho = 1.25$. We obtain $\mathcal{R}_0 = 2.5572$.

5. Conclusion

In this paper, we developed a simple SIR mathematical model of the coronavirus disease 2019. And by considering reported data for Burkina Faso, we address the epidemiological effect of delay in hospitalisation that is also related to the weakness of the health system and a complex humanitarian and security crisis the country had been facing since 2015 [21, 38]. The basic reproduction number of the model system $\mathcal{R}_0$ has been computed and we have derived some necessary conditions for the local and global stability of the model steady states. We also performed a local sensitivity analysis of $\mathcal{R}_0$, to show how each parameter of the model is affecting the disease dynamics [12, 19, 23]. However, since the $\mathcal{R}_0 < 1$ is not sufficient for the disease disappearance from the population, we have studied the backward bifurcation and we found that ρ which accounts for the delay in management is an important parameter for the bifurcation occurrence [5, 7, 16, 32]. Our results show that the limited availability of medical resources has favoured the emergence of complex dynamics that accelerated the outbreak the COVID-19 disease in Burkina Faso, [17, 20]. In short, this work addresses a critical issue related to the COVID-19 pandemic, focusing on the impact of a precarious health system on the disease's transmission dynamics in Burkina Faso. The study's relevance is heightened by its applicability to other developing countries with similar health system challenges. The COVID-19 pandemic, that has shaken the world, remains a textbook case. Countries around the world, especially developing ones, must be prepared for such infectious disasters,[6, 14, 21, 33, 35]. This includes strengthening health systems, strengthening collaboration between

these systems, preparing populations to change their community habits if necessary for the common good, strengthening resources and information channels, [12, 14, 21, 35].

Acknowledgement. The authors would like to express their sincere thanks to the associate editor and the anonymous referees for their constructive comments.

Furthermore, the first author Ousmane KOUTOU would like to thank Dr Ramsès DJIDJOU-DEMASSE from IRD-Montpelier (France) and Dr Ousmane SEYDI from École Polytechnique de Thiès (Senegal) for their useful advices and supports.

Authors' contributions All authors have worked together to produce the paper and have read and approved the final version of it.

Funding Not applicable.

Availability of data Not applicable.

Competing interests The authors declare that there is any conflict of interest about the publication of this work.

References

1. https://en.wikipedia.org/wiki/COVID-19_pandemic_in_Burkina_Faso#Confirmed_new_cases_per_day
2. https://en.wikipedia.org/wiki/COVID-19_pandemic_in_Italy#Timeline
3. https://www.who.int/health-topics/coronavirus
4. https://www.worldometers.info/coronavirus/country/Burkina-Faso/
5. K. Alanazi, Traveling wave solutions of a susceptible-infectious model. *Annals of Mathematics and Computer Science*, Vol. **24**, No. 7, (2024), pp. 117 – 126. https://doi.org/10.56947/amcs.v24.354
6. R. T. Alqahtani, A. Ajbar, Study of dynamics of a COVID-19 model for Saudi Arabia with vaccination rate, saturated treatment function and saturated incidence rate, *Mathematics*, Vol. **9**, No. 23, (2021), pages 3134. Mathematics2021,9(23),3134;https://doi.org/10.3390/math9233134
7. J. K. K. Asamoah, M. A. Owusu, Z. Jin, F. T. Oduro, A. Abidemi & E. O. Gyasi, Global stability and cost-effectiveness analysis of COVID-19 considering the impact of the environment: using data from Ghana, *Chaos Solitons Fractals*, Vol. **140**, (2020). https://doi:10.1016/j.chaos.2020.110103
8. G. Birkhoff & G.-C. Rota, Ordinary differential equations, Ginn, Boston, (1982). https://archive.org/details/ordinarydifferen0000birk_f0p6
9. J. Carr, Applications Centre Manifold Theory, Springer-Verlag, New York, (1981). https://doi.org/10.1007/978-1-4612-5929-9
10. C. Castillo-Chavez & B. Song, Dynamical models of tuberculosis and their applications, *Math. Biosci. Eng.*, Vol. **1**, No. 2, (2004), pp. 361 – 404. https://doi:10.3934/mbe.2004.1.361
11. A. B. Diabaté, B. Sangaré & O. Koutou, Mathematical modeling of the dynamics of vector-borne diseases transmitted by mosquitoes : taking into account aquatic stages and gonotrophic cycle, *Nonauton. Dyn. Syst.*, Vol. **9**, No. 1, (2022), pp. 205 – 236. https://doi.org/10.1515/msds-2022-0155

12. A. B. Diabaté, B. Sangaré & O. Koutou, Optimal control analysis of a COVID-19 and Tuberculosis (TB) co-infection model with an imperfect vaccine for COVID-19, *SeMA Journal*, (2023). https://doi.org/10.1007/s40324-023-00330-8
13. S. E. Eikenberry, M. Mancuso, E. Iboi, T. Phan, K. Eikenberry, Y. Kuang, E. Kostelich, A. B. Gumel, To mask or not to mask: Modeling the potential for face mask use by the general public to curtail the COVID-19 pandemic, *Infectious Disease Modelling*, Vol. **5**, (2020), pp. 293 – 308. https://doi.org/10.1016/j.idm.2020.04.001
14. J. K. Ghosh, S. K. Biswas, S. Sarkar & U. Ghosh, Mathematical modelling of COVID-19: A case study of Italy, *Math. Comput. Simul.*, Vol. **194**, (2022), pp. 1 – 18. doi.org/10.1016/j.matcom.2021.11.008
15. N. K. Goswami, S. Olaniyi, S. F. Abimbade & F. M. Chuma, A mathematical model for investigating the effect of media awareness programs on the spread of COVID-19 with optimal control, *Healthcare Analytics*, (2024). https://doi.org/10.1016/j.health.2024.100300
16. A. Guiro, B. Koné and S. Ouaro, Mathematical model of the spread of the coronavirus disease 2019 (COVID-19) in Burkina Faso, *Applied Mathematics*, Vol. **11**, (2020), pp. 1204– 1218. https://doi.org/10.4236/am.2020.1111082
17. A. Guiro, B. Koné & S. Ouaro, Mathematical Modelling of the Evolution Dynamics of the Coronavirus Disease 2019 (COVID-19) in Burkina Faso, *Toni, B. (eds) The Mathematics of Patterns, Symmetries, and Beauties in Nature. STEAM-H: Science, Technology, Engineering, Agriculture, Mathematics & Health. Springer, Cham.*, (2021). https://doi.org/10.1007/978-3-030-84596-4_6
18. J. K. Hale, Ordinary differential equations, *New York: Wiley*, (1969). https://learn.fmi.uni-sofia.bg/pluginfile.php/200162/mod_resource/content/0/Hale%20-%20Ordinary%20Differential%20Equations.pdf
19. S. M. Kassa, J. B. H. Njagarah & Y. A. Terefe, Modelling COVID-19 mitigation and control strategies in the presence of migration and vaccination: the case of South Africa, *Afr. Mat.*, (2021). https://doi.org/10.1007/s13370-021-00900-x
20. F. V. Konané & A. Traoré, Statistical modeling and forecast of the coronavirus disease (COVID-19) in Burkina Faso, *International Journal of Statistics and Probability*, Vol. **9**, No. 6, (2020). https://doi.org/10.5539/ijsp.v9n6p76
21. O. Koutou, A. B. Diabaté and B. Sangaré, Mathematical analysis of the impact of the media coverage in mitigating the outbreak of COVID-19, *Math. Comput. Simul.*, Vol. **205**, (2023), pp. 600 – 618. https://doi.org/10.1016/j.matcom.2022.10.017
22. O. Koutou, B. Sangaré & A. B. Diabaté, Mathematical analysis of mosquito population global dynamics using delayed-logistic growth, *Malaya J. Math.*, Vol. **8**, No. 4, (2020), pp. 1898 – 1905. https://doi.org/10.26637/MJM0804/0094
23. O. Koutou, B. Traore & B. Sangare, Analysis of schistosomiasis global dynamics with general incidence functions and two delays, *Int. J. Appl. Comput. Math.*, Vol. **7**, No. 245, (2021). https://doi.org/10.1007/s40819-021-01188-y
24. J. P. LaSalle, The Stability of Dynamical Systems, *Regional Conference Series in Applied Mathematics, SIAM, Philadelphia,* (1976). https://doi.org/10.1137/1.9781611970432
25. P. Magal, A COVID-19 Epidemic Model with Latency Period, 2020, Available at SSRN: https://ssrn.com/abstract=3558797.
26. M. Martcheva, An introduction to mathematical epidemiology, New York: Springer, Vol. **61**, (2015), pp. 9 – 31.https://doi.org/10.1007/978-1-4899-7612-3
27. Bimal K. Mishra, A. K. Keshri, D. K. Saini, S. Ayesha, Binay Mishra, Y. S. Rao, Mathematical model, forecast and analysis on the spread of COVID-19, *Chaos Solitons Fractals,* Vol. **147**, (2021), pages 110995. https://doi.org/10.1016/j.chaos.2021.110995
28. J-P. Moatti, The French response to COVID-19: intrinsic difficulties at the interface of science, public health, and policy, *The Lancet Public Health*, Vol. **5**, No. 5, (2020). https://doi.org/10.1016/S2468-2667(20)30087-6

29. Mohanapriya, A. Stability analysis of linear quaternion-valued differential equation using integral transform, *Annals of Mathematics and Computer Science*, Vol. **22**, No. 7, (2024), pp. 88 – 99. https://doi.org/10.56947/amcs.v22.274
30. Z. Mukandavire, A. B. Gumel, W. Garira & J. M. Tchuenche, Mathematical analysis of a model for HIV-Malaria co-infection, *Math. Biosci. Eng.*, Vol. **6**, No. 2, (2009), pp. 333 – 362. https://doi.org/10.3934/mbe.2009.6.333
31. I. I. Oke, Y. T. Oyebo, O. F. Fakoya, V. S. Benson & Y. T. Tunde, A mathematical model for COVID-19 disease transmission dynamics with impact of saturated treatment: modeling, analysis and simulation, *Open Access Library Journal*, Vol. **8**, No. 5, (2021), pp. 1 – 20. https://doi.org/10.4236/oalib.1107332
32. Olabanjo, O. & Wusu, A. Dynamics of sustainable fisheries: a mathematical approach using Lotka-Volterra equations, *Annals of Mathematics and Computer Science*, Vol. **19**, No. 6, (2023), pp. 59 – 67. https://doi.org/10.56947/amcs.v19.225
33. D. A. Oluyori, Á. G. C. Pérez, V. A. Okhuese & M. Akram, Backward and Hopf bifurcation analysis of an SEIRS COVID-19 epidemic model with saturated incidence and saturated treatment response, *medRxiv*, (2020). https://doi.org/10.1101/2020.08.28.20183723
34. H. Ouédraogo & A. Traoré, Global properties of a delayed vector-borne disease model with partial protection of susceptible humains, *Differ. Equ. Dyn. Syst.*, (2023), pp. 1 – 17. https://doi.org/10.1007/s12591-023-00652-z
35. P. Saha, S. K. Biswas, M. H. A. Biswas & U. Ghosh, An SEQAIHR model to study COVID-19 transmission and optimal control strategies in Hong Kong, 2022, *Nonlinear dyn.*, Vol. **111**, No. 7, (2023), pp. 6873–6893. https://doi.org/10.1007/s11071-022-08181-0
36. A. Savadogo, H. Ouedraogo, B. Sangare, W. Ouedraogo, Mathematical analysis of a fish-plankton eco-epidemiological system, *Nonlinear Studies*, Vol. **27**, No. 1, pp. 237 – 261, (2020). https://https://www.researchgate.net/publication/361441385_Mathematical_analysis_of_a_fish-plankton_eco-epidemiological_system
37. A. Traoré, Analysis of a vector-borne disease model with human and vectors immigration, *J. Appl. Math. Comput.*, Vol. **64**, (2020), pp. 411–428. https://doi.org/10.1007/s12190-020-01361-4
38. A. Traoré & F. V. Konané, Modeling the effects of contact tracing on COVID-19 transmission. *Adv. Differ. Equ.* Vol. **2020**, No. 509, (2020). https://doi.org/10.1186/s13662-020-02972-8
39. S. Y. Tchoumi, M. L. Diagne, H. Rwezaura & J. M. Tchuenche, Malaria and COVID-19 co-dynamics: A mathematical model and optimal control, *Appl. Math. Model.*, Vol. **99**, (2021), pp. 294 – 327. https://doi.org/10.1016/j.apm.2021.06.016
40. B. Traoré, O. Koutou & B. Sangaré, A global mathematical model of malaria transmission dynamics with structured mosquito population and temperature variations, *Nonlinear Anal. Real World Appl.*, Vol. **53**, No. 103081, (2020). https://doi.org/10.1016/j.nonrwa.2019.103081
41. J. Zhang, J. Jia & X. Song, Analysis of an SEIR epidemic model with saturated incidence and saturated treatment function, *Scientific World Journal*, Vol. **2014**, (2014), ID 910421. https://doi.org/10.1155/2014/910421
42. X. Zhou & J. Cui, Analysis of stability and bifurcation for an SEIR epidemic model with saturated recovery rate, *Commun. Nonlinear Sci. Numer. Simul.*, Vol. **16**, No. 11, (2011), pp. 4438 – 4450. https://doi.org/10.1016/j.cnsns.2011.03.026

[1] CU-Kaya/ Université Joseph KI-ZERBO, 03 BP 7021 Ouagadougou 03, Burkina Faso.
Email address: koutousman@gmail.com/koutou@um.es

[2] Department of Mathematics and Applied Mathematics, University of the Free State, QwaQwa Campus, South Africa.
Email address: komia@aims.ac.za/afassinouk@ufs.ac.za

[3,4] Département de mathématiques, Université Nazi BONI, 01 BP 1091 Bobo-Dioulasso 01, Burkina Faso.

Email address: [3]adam.ouedraogo3@yahoo.fr and [4]diaboubakre@gmail.com